

# Simultaneous observations of maser lines of $^{28}\text{SiO}$ in evolved stars

J.R. Pardo<sup>1,2,3</sup>, J. Cernicharo<sup>4,2</sup>, E. González-Alfonso<sup>5,2</sup>, and V. Bujarrabal<sup>2</sup>

<sup>1</sup> DEMIRM/Observatoire de Paris-Meudon, 61 Avenue de l'Observatoire, F-75014 Paris, France

<sup>2</sup> Observatorio Astronómico Nacional, Campus Universitario Apartado 1143, E-28800 Alcalá de Henares, Madrid, Spain

<sup>3</sup> Present address: NASA-Goddard Institute for Space Studies, 2880 Broadway, New York, NY 10025, USA

<sup>4</sup> CSIC, IEM, Dpto. Física Molecular, Serrano 123, E-28006 Madrid, Spain

<sup>5</sup> Universidad de Alcalá de Henares, Departamento de Física, Campus Universitario, E-28871 Alcalá de Henares, Madrid, Spain

Received 21 May 1997 / Accepted 7 August 1997

**Abstract.** We present simultaneous observations of several rotational lines of  $^{28}\text{SiO}$  in the  $v=1, 2, 3$ , and 4 vibrationally excited states toward O-rich evolved stars. All the data were taken in a relatively short period of 65 days, which allows a comparative study of the  $^{28}\text{SiO}$  maser lines intensities and profiles.

The observed differences concerning intensity and line shape among the different maser lines suggest that infrared overlaps deeply affect the pumping of some SiO masers. We qualitatively discuss this effect with consideration to the IR overlaps at 8  $\mu\text{m}$  between the various SiO isotopomers and between  $^{28}\text{SiO}$  and water vapor <sup>1</sup>.

**Key words:** stars: AGB, post-AGB – masers – stars: circumstellar matter – radio-lines: stars

## 1. Introduction

Maser emission in  $^{28}\text{SiO}$  rotational transitions of vibrationally excited states is currently observed in evolved O-rich stars. Rotational transitions up to  $J = 7 \rightarrow 6$  have been detected in the  $v=1, 2, 3$  and 4 vibrational states (Jewell et al. 1987, Gray et al. 1995, Cernicharo et al. 1993, and references therein). A certain number of maser lines have been also detected in the ground and excited vibrational states of the rare isotopomers  $^{29}\text{SiO}$  and  $^{30}\text{SiO}$  (e.g. Deguchi et al. 1983, Cernicharo et al. 1991, Alcolea & Bujarrabal 1992, Cernicharo & Bujarrabal 1992, González-Alfonso et al. 1996).

Despite of the large amount of observational data that can be found in literature, SiO maser emission presents some conspicuous aspects that require further observational and theoretical effort. Besides the overall inversion of the rotational transitions

in each vibrational ladder, the SiO emission displays anomalies in some rotational lines, i.e., drastic changes in intensity from one rotational line to the next of the same  $v$ -state. Although the general inversion process seems to be relatively well understood (see e.g. Bujarrabal 1994-I-II), those differences in the emission of adjacent rotational lines are difficult to explain upon standard (radiative or collisional) pumping models. Such anomalies, which are particularly important for the high- $v$  states of  $^{28}\text{SiO}$  also apply to the rare isotopomers  $^{29}\text{SiO}$  and  $^{30}\text{SiO}$  in  $v=0, 1, 2$  and 3. They have been interpreted as being produced by overlaps between the ro-vibrational lines of the  $^{28}\text{SiO}$ ,  $^{29}\text{SiO}$  and  $^{30}\text{SiO}$  (Cernicharo et al. 1991, Cernicharo and Bujarrabal 1992, Cernicharo et al. 1993). González-Alfonso & Cernicharo (1997) have successfully explained qualitatively most of the maser lines of SiO rare isotopic species upon the basis of the proposed IR overlaps. Simultaneous observations of  $^{29}\text{SiO}$  and  $^{30}\text{SiO}$  rotational lines will be presented by González-Alfonso et al. (1998). In addition to these IR overlaps, another one between SiO and H<sub>2</sub>O has been proposed to explain the  $v=2$   $J=2-1$  line of  $^{28}\text{SiO}$  (Olofsson et al. 1981, Olofsson 1985, Langer & Watson 1984, Bujarrabal et al. 1996).

Except for the observation of 11 lines of  $^{28}\text{SiO}$  in 6 evolved stars by Schwartz et al. (1982), the line survey in the red supergiant VY CMa by Cernicharo et al. (1993), and the source survey by Cho et al. (1996) of six  $J = 1 \rightarrow 0$  transitions in various vibrational states of  $^{28}\text{SiO}$  and  $^{29}\text{SiO}$ , most of the observational studies of the SiO maser emission have been carried out in different epochs and with different instruments. Unfortunately, due to the variability of the SiO maser emission, observations taken in different periods cannot be compared to infer reliable conclusions about the excitation of SiO. In order to proceed further in the resolution of the SiO excitation problem, it seems necessary to obtain the most complete and time-homogeneous observations of the SiO rotational emission in the different  $v$ -states.

In this paper we present observations of several  $^{28}\text{SiO}$  maser lines (see Table 1) in the direction of 12 O-rich evolved stars (listed in Table 2). The most complete set of observations was achieved for R Leo, two months after its strong maximum of

Send offprint requests to: J.R. Pardo

<sup>1</sup> Tables 5 to 16 are only available in electronic form at the CDS via anonymous ftp to cdsarc.u-strasbg.fr (130.79.128.5) or via <http://cdsweb.u-strasbg.fr/Abstract.html>.

1992 September 12-15 (observed in detail by Pijpers et al. (1994) in the  $^{28}\text{SiO}$   $v=1,2$   $J=1-0$  lines). We observed towards this star a total of 17 lines, and 10 of them were detected. The number of transitions detected in the rest of sources was between 4 and 10 (see Figs. 1 to 6).

We have organized this paper as follows. The instruments and the observational technique are described in section 2. Section 3 is devoted to the presentation of results. A qualitative discussion of the effect of some couples of IR overlapped lines (belonging to  $^{28,29,30}\text{Si}^{16}\text{O}$  and  $\text{H}_2^{16}\text{O}$ ) on the observed excitation anomalies is given in section 4. Finally, we summarize the most important conclusions of this work in section 5.

## 2. Instruments and observations

The observations were carried out in 1992 November 14-15, and in 1993 January 26-27. The difference of two months between the two observing runs is short enough to allow comparison of line shapes and intensities, provided that the pulse periods of these stars are much longer. All the observations were carried out with the 30-m IRAM radiotelescope located on Pico Veleta (Spain), except for the  $J=1\rightarrow 0$ ,  $v=1,2,3$  lines that were observed with the 13.7-m radiotelescope at the Centro Astronómico de Yebes (Spain).

The Mira-type stars R Cas, NML Tau and R Leo were observed close to their  $^{28}\text{SiO}$   $v=1,2$   $J=1\rightarrow 0$  respective maxima (the SiO maximum emission appears to be shifted with a phase lag of 0.1-0.3 relative to the visual maximum; e.g., Martínez et al. 1988, Alcolea 1992 and Alcolea et al. 1997). The phases given by the AAVSO for the three cited stars at 1992 November 15 were 0.32, 0.32 and 0.24 respectively. Other objects were observed near the  $v=1,2$   $J=1\rightarrow 0$  minimum (TX Cam, for example, was observed at a phase of  $\sim 0.75$ ).

The observed  $^{28}\text{SiO}$  transitions, together with their frequencies, are listed in Table 1. We attempted to observe some rotational lines within the  $v=4$  state in R Leo, S Per,  $\mu$  Cep, NML Cyg, R Aql, R Cas and RR Aql, with negative results for all them (see non-detection limits in Table 3). Search for emission in the  $^{28}\text{SiO}$   $v=5$   $J=2-1$  line towards R Leo and R Aql was not either successful.

The observations at the 30-m telescope made use of three SIS receivers working at the 1.3 mm, 2 mm and 3 mm atmospheric windows between the strong telluric absorptions of  $\text{O}_2$  at 60 and 118.8 GHz and of  $\text{H}_2\text{O}$  at 183.3 and 325 GHz. An open structure SIS receiver, working in the region of frequencies around 350 GHz, was also tuned at the frequencies of  $^{28}\text{SiO}$   $J=8\rightarrow 7$   $v=1,2,3,4$  lines. At these frequencies, the atmospheric transmission at the altitude of the IRAM-30m telescope is  $\sim 60\%$  under typical winter time conditions. The main beam single sideband (SSB) system temperatures were typically 900, 400, 300 and 1600 K for the 1.3 mm, 2 mm, 3 mm and 350 GHz receivers, respectively. The spectrometers connected to these receivers were a 512x1MHz filter bank, a 256x100kHz filter bank, and an autocorrelator with 1024 channels and a total bandwidth of 20 MHz. The pointing was monitored every 30 minutes towards the observed star by using a Schottky receiver tuned at the fre-

**Table 1.** Observed  $^{28}\text{SiO}$  transitions

v	J	central freq. (MHz)
1	1 $\rightarrow$ 0	43122.024
1	2 $\rightarrow$ 1	86243.362
1	3 $\rightarrow$ 2	129363.259
1	4 $\rightarrow$ 3	172481.014
1	5 $\rightarrow$ 4	215595.914
1	6 $\rightarrow$ 5	258707.246
1	8 $\rightarrow$ 7	344934.678
2	1 $\rightarrow$ 0	42820.534
2	2 $\rightarrow$ 1	85640.397
2	4 $\rightarrow$ 3	171275.076
2	5 $\rightarrow$ 4	214088.485
2	8 $\rightarrow$ 7	342504.407
3	1 $\rightarrow$ 0	42519.380
3	2 $\rightarrow$ 1	85037.997
3	4 $\rightarrow$ 3	170070.267
3	5 $\rightarrow$ 4	212582.465
3	8 $\rightarrow$ 7	340158.672
4	2 $\rightarrow$ 1	84436.159
4	4 $\rightarrow$ 3	168866.583
4	5 $\rightarrow$ 4	211077.852
4	8 $\rightarrow$ 7	337642.672
5	2 $\rightarrow$ 1	83834.851

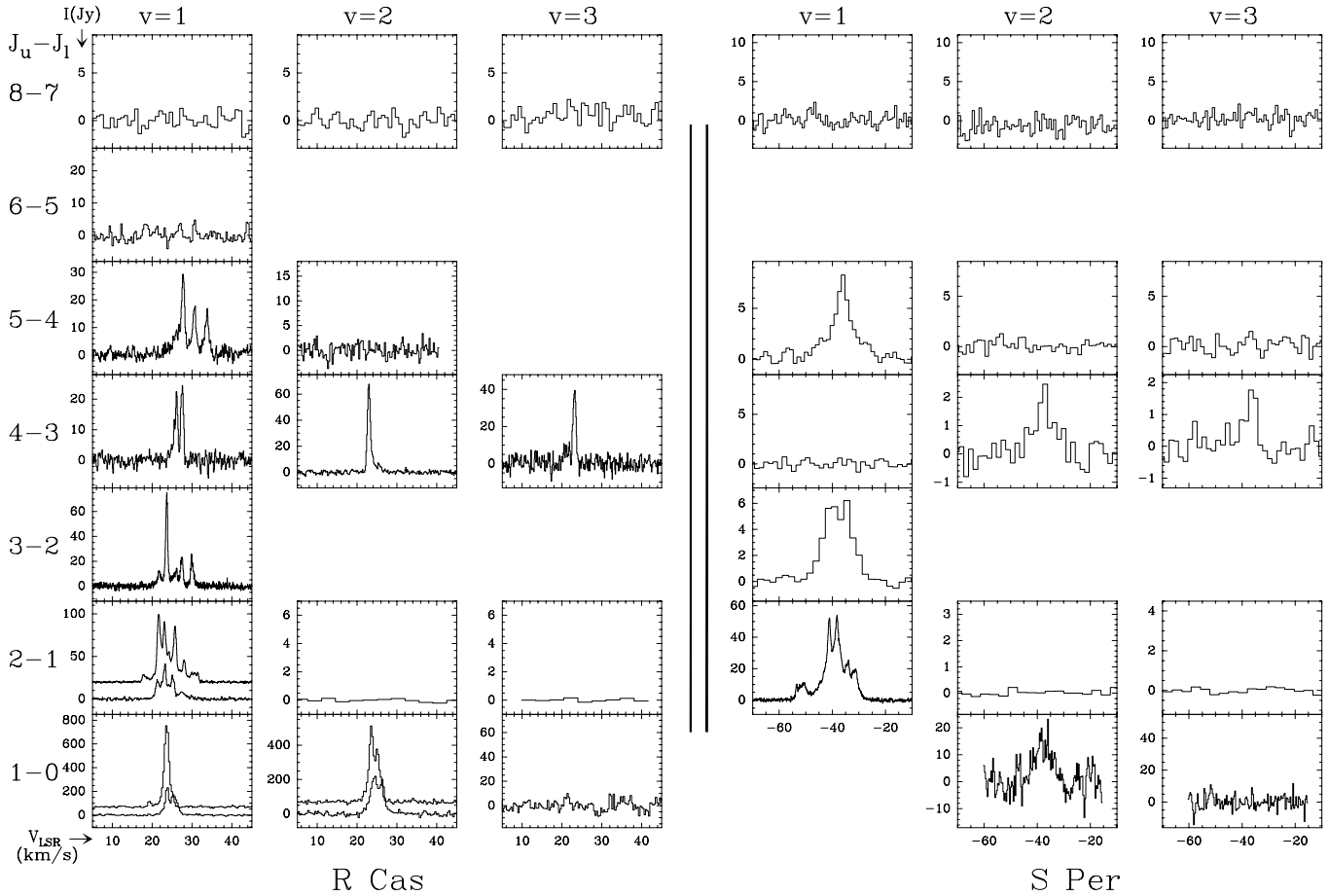
quency of the strong  $^{28}\text{SiO}$   $v=1$   $J=2\rightarrow 1$  maser. This line was also used to check the focusing of the telescope. The relative pointing accuracy of the five receivers was better than  $2''$ . The 1mm, 2mm and 3mm receivers are only sensible to a linear polarization component on the sky, which is crossed for the 2mm receiver relative to the other two. Observations were made with a wobbler system that provided very good baselines. The antenna temperature scale was achieved upon calibration of the signal with the use of two absorbents at different temperatures. Sky opacities were derived from measurements of the sky emissivity and the atmospheric model ATM (Cernicharo 1985, 1988; see also Pardo 1996). The factors to transform main-beam antenna temperatures in Janskys are 4.5, 5.0, 6.0 and 1.2 for the 3mm, 2mm, 1.3mm and 350 GHz receivers, respectively.

The 13.7-m radiotelescope of the Centro Astronómico de Yebes was equipped during the observations with a cooled Schottky receiver. The SSB system temperature was typically 260 K. The back-end was a 256x50kHz filter bank. A polarizer was installed in front of the receiver allowing the observation of circular polarization. The frequency switching mode was used during these observations. In order to measure and correct for pointing effects, the observations on each source consisted of several small maps of five points, one at the expected position of the star and the others at offset positions of  $30''$ . The atmospheric absorption, almost exclusively due to oxygen at the frequency of 43 GHz, is estimated to be 7 % at the position of the telescope.

The list of observed stars, together with their coordinates and their spectral and variability type (from Kholopov et al., 1985) are given in Table 2.

**Table 2.** Observed objects

name	observation coordinates		spectral type	variability type	comments
	$\alpha$ (1950)	$\delta$ (1950)			
IRC+10011	01 03 48.0	+12 19 51	M8	mira	WX Psc
S Per	02 19 15.1	+58 21 34	M5		supergiant
IK Tau	03 50 43.6	+11 15 32	M6-M10	mira	NML Tau
TX Cam	04 56 43.0	+56 06 48	M8-M10	mira	
IRC+50137	05 07 19.7	+52 48 54	M10	mira	NV Aur
R Leo	09 44 52.2	+11 39 40	M6-M9	mira	
R Aql	19 03 57.7	+08 09 08	M5	mira	
RR Aql	19 55 00.3	-02 01 17	M6	mira	
NML Cyg	20 44 33.8	+39 55 57		SRc	supergiant
T Cep	21 08 52.7	+68 17 10	M5	mira	supergiant
$\mu$ Cep	21 41 58.5	+58 33 01	M2		supergiant
R Cas	23 55 52.0	+51 06 37	M6-M10	mira	

**Fig. 1.** Observations of SiO rotational lines in R Cas and S Per. Most of the observations were achieved during November 1992 and some others in January 1993.

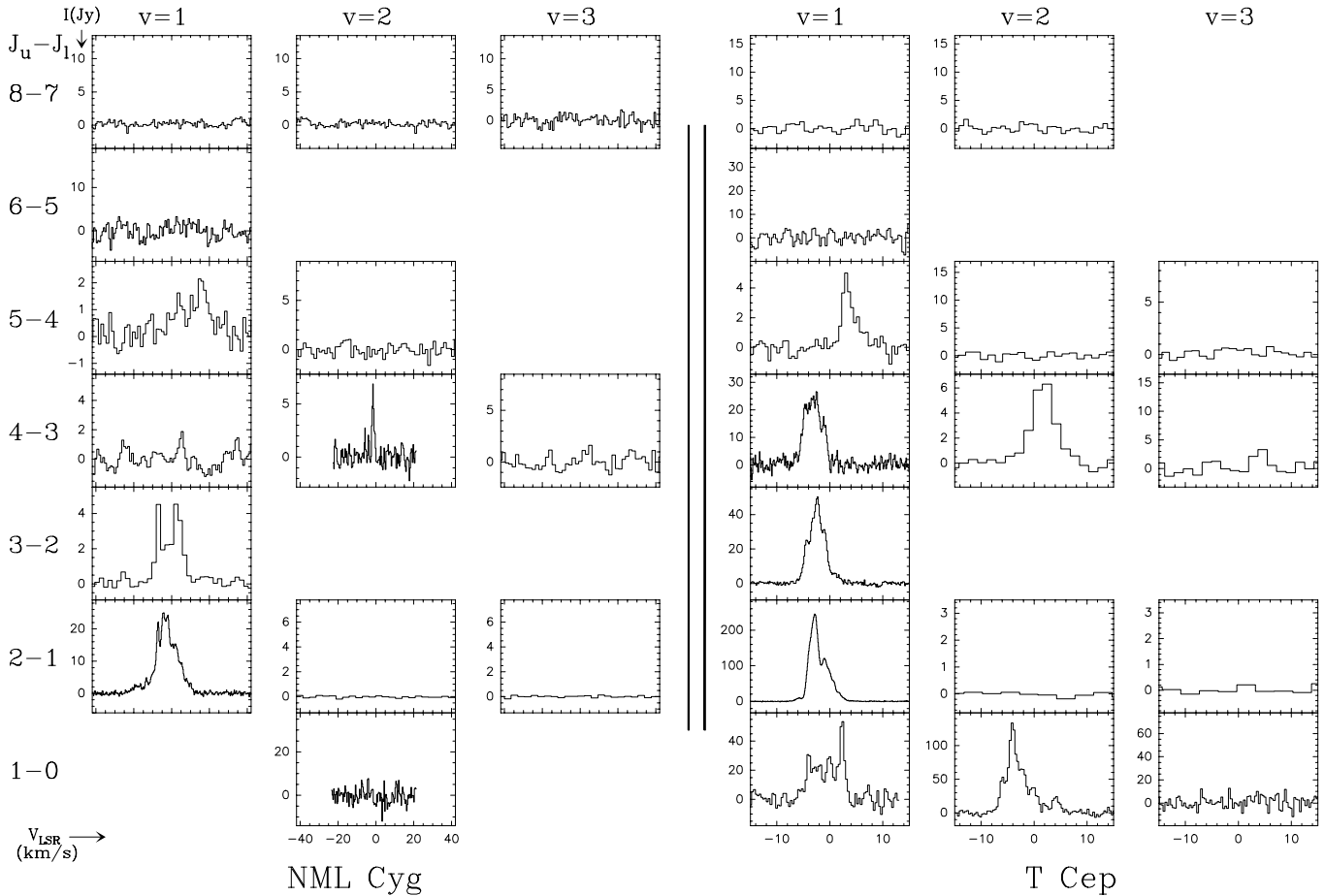


**Fig. 2.** Simultaneous observations of SiO rotational lines in NML Cyg and T Cep. For T Cep most of the observations were achieved during November 1992 and a few in January 1993.

### 3. Results

Figs. 1-6 show most of the observations carried out in the 12 stars of our sample; only a few non-detected lines are not displayed. In particular, our SiO line survey included observations of the  $v=1,2,3,4$   $J=8\rightarrow7$  lines, which were not detected in any source. The rms noise in the spectra of the undetected lines is given in Table 3. We have fitted gaussian curves to the detected lines. Tables 5 to 16 (available only in electronic form) list the fitted peak velocity, line width at half power, and velocity-integrated intensity.

Inspection of Figs. 1 to 6 reveals that, in general, the line profiles and the velocity of the spectral features corresponding to transitions in different  $v$ -states do not coincide. The cases of peak coincidence between lines of different  $v$ -states are rare. Such variations are expected from theoretical model calculations which predict (e.g. Cernicharo et al 1991, Bujarrabal 1994-I-II) that the masers arising in different  $v$ -states require different physical conditions to pump, so that they are formed in distinct regions with various kinematical properties. More conspicuous are, however, the lack of similarity between the line profiles corresponding to rotational transitions of the same  $v$ -state, and that can be observed in some sources (Figs. 1 to 6). They cannot

be explained on the basis of the standard pumping models, thus we shall refer to them as anomalies. It will be shown below that IR overlaps are probably necessary to explain such phenomena.

From the observed line profiles we extract a number of conclusions, summarized in the following sections.

#### 3.1. $^{28}\text{SiO}$ rotational lines in $v=1$

Most of the observed  $^{28}\text{SiO}$  lines within  $v=1$ , up to  $J=5\rightarrow4$ , are relatively strong masers, with an integrated intensity that varies smoothly from one rotational line to the next. The maximum flux is usually found in the  $J=2\rightarrow1$  line. However, the line profiles in some stars show individual spectral features with strong intensity variations from one rotational transition to the next. The whole line profile also change appreciably with  $J$  in some objects, like R Cas. The  $J=5\rightarrow4$  line presents the most anomalous behavior within the  $v=1$  vibrational state. In R Cas, for example, the line profile shows a spike at  $34 \text{ km s}^{-1}$  which has no counterpart in any other transition. It is also remarkable the presence of a spectral component at  $3.4 \text{ km s}^{-1}$  in the  $v=1$   $J=5\rightarrow4$  transition of T Cep, whereas no emission at that velocity is found in the  $J=1\rightarrow0$ ,  $2\rightarrow1$ ,  $3\rightarrow2$  and  $4\rightarrow3$  lines. Finally,

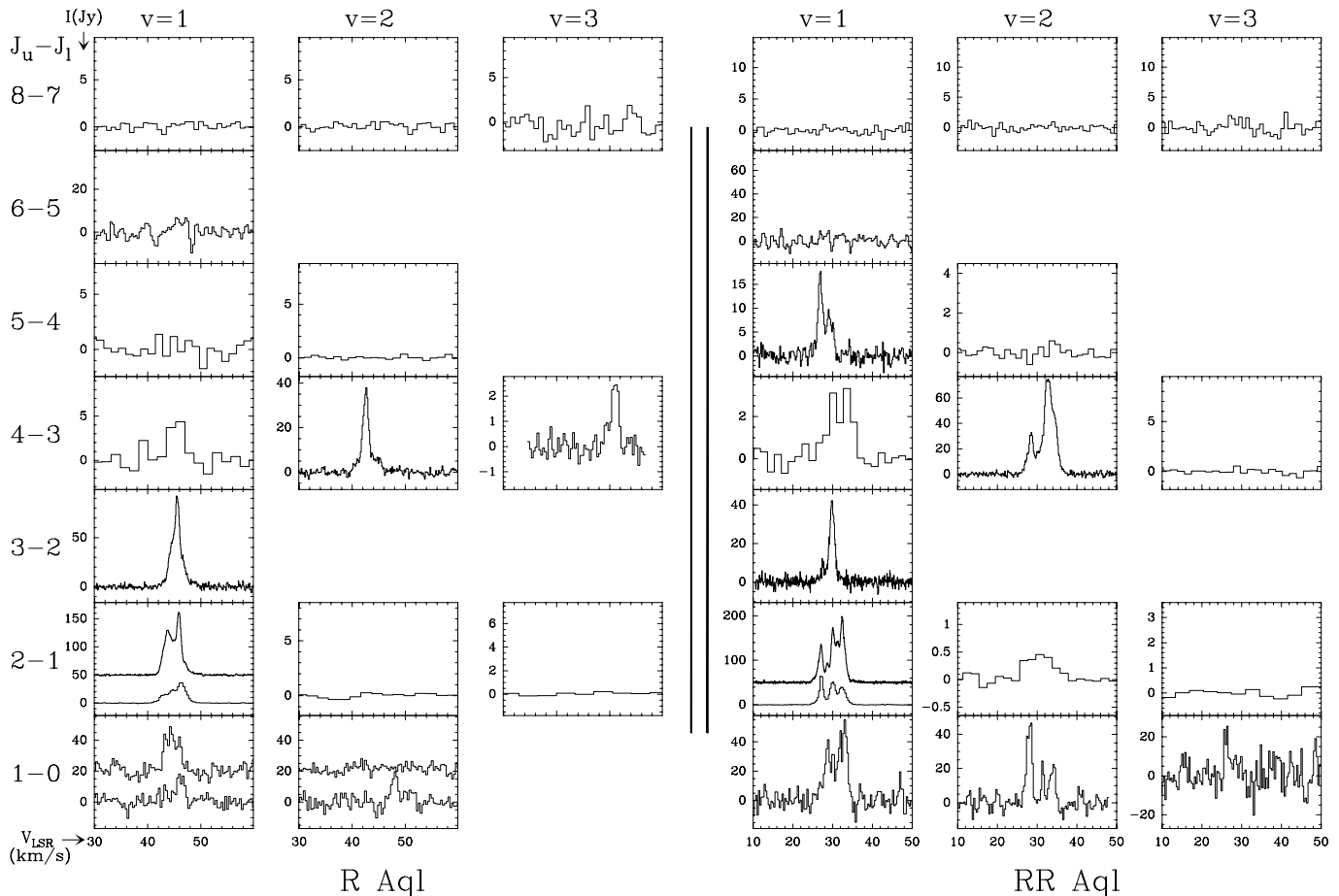


**Fig. 3.** Observations of SiO rotational lines in R Aql and RR Aql. Most of the observations were achieved during November 1992 and some others in January 1993.

we point out the case of S Per, where the  $v=1$   $J=4 \rightarrow 3$  transition shows no emission whereas the  $J=3 \rightarrow 2$  and  $J=5 \rightarrow 4$  lines are detected, as well as the case of RR Aql where the emission in  $v=1$   $J=4 \rightarrow 3$  is around 10 times weaker than in  $J=3 \rightarrow 2$  and  $J=5 \rightarrow 4$ . These facts are hardly compatible with predictions of simple models, which indicate that the different rotational lines in a given  $v$ -state are almost simultaneously inverted.

Nevertheless, the above situation is not common to all the observed stars. We note that IK Tau and R Aql show similar line profiles for all the rotational transitions within  $v=1$ . The  $v=1$  lines in IK Tau have a main peak centered at  $34 \text{ km s}^{-1}$  with smooth intensity variations from one rotational transition to the next.

### 3.2. $^{28}\text{SiO}$ rotational lines in $v=2,3,4$ and 5

It is very hard to detect rotational lines within the  $v=3,4$  and 5 states, most probably due to the high energy of the levels involved in these transitions. An exception to this rule is the  $v=3$   $J=4 \rightarrow 3$  line, which has been effectively detected in several objects. We can mention earlier detections of lines in the  $v=3$  state, as the  $J=1 \rightarrow 0$  maser line (e.g. Alcolea et al. 1989),

which was detected in most of the objects presented in this work, a tentative detection of  $v=3$ ,  $J=5 \rightarrow 4$  in the red supergiant VX Sgr (Jewell et al. 1987), and the detection of the  $v=4$   $J=5-4$  line by Cernicharo et al. (1993) in the red supergiant VY CMa. The integrated line intensity of the various rotational lines within these vibrational states does not show a regular pattern of variation.

It is remarkable that the total velocity coverage of the detected  $v=2$  and  $v=3$  lines towards R Leo is larger than in the corresponding  $v=1$  transitions. The total velocity dispersion for this star attains almost  $20 \text{ km s}^{-1}$  in some lines. This value is appreciably larger than the dispersion of the thermal CO lines (Cernicharo et al 1994, 1997), i.e., the high- $v$  SiO lines of R Leo originate in regions where the velocity dispersion is significantly larger than the expansion velocity characteristic of the external circumstellar layers. However, most sources within our sample do not show such a behavior. R Cas (in which the detected lines show the richest structure among the observed objects) and  $\mu$  Cep are examples of the opposite situation, with the  $v=1$  masers significantly broader than the  $v=2$  and  $v=3$  ones. The high velocity dispersion observed in R Leo is difficult to explain in terms of expanding circumstellar dynamics, so that

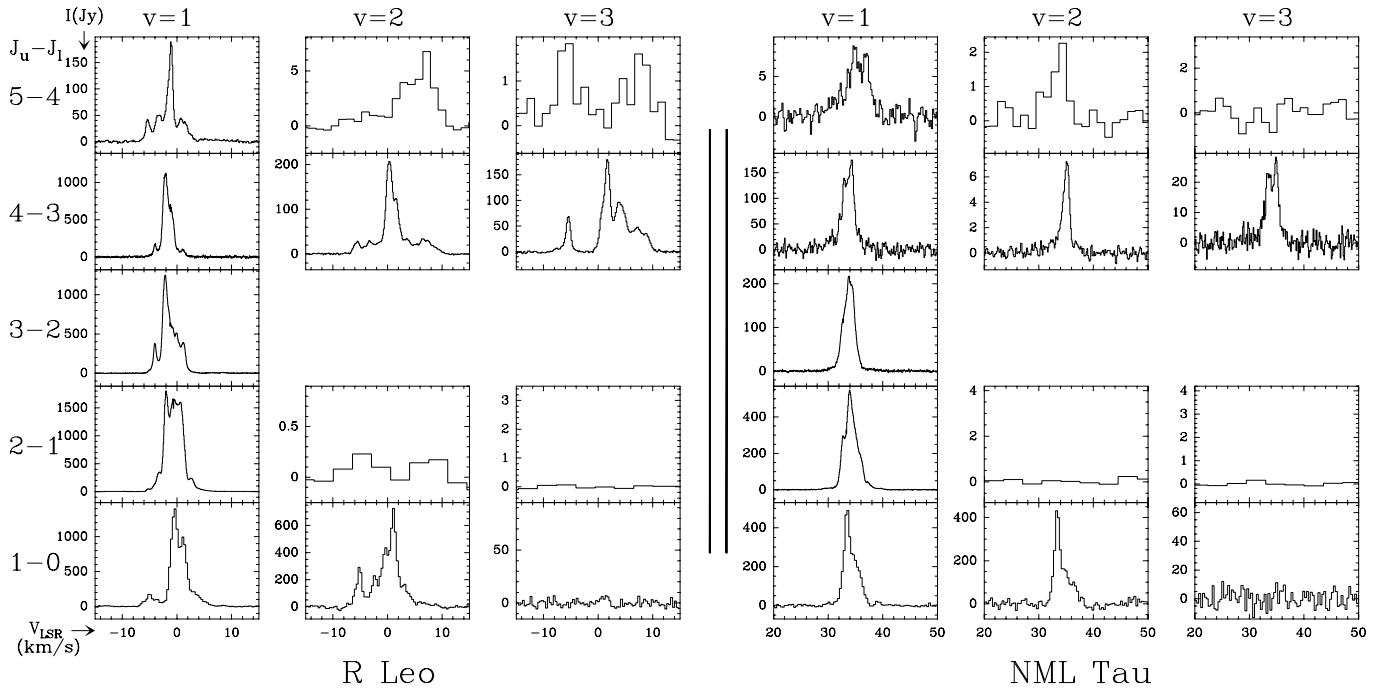


**Fig. 4.** Simultaneous observations of SiO rotational lines in R Leo and NML Tau.

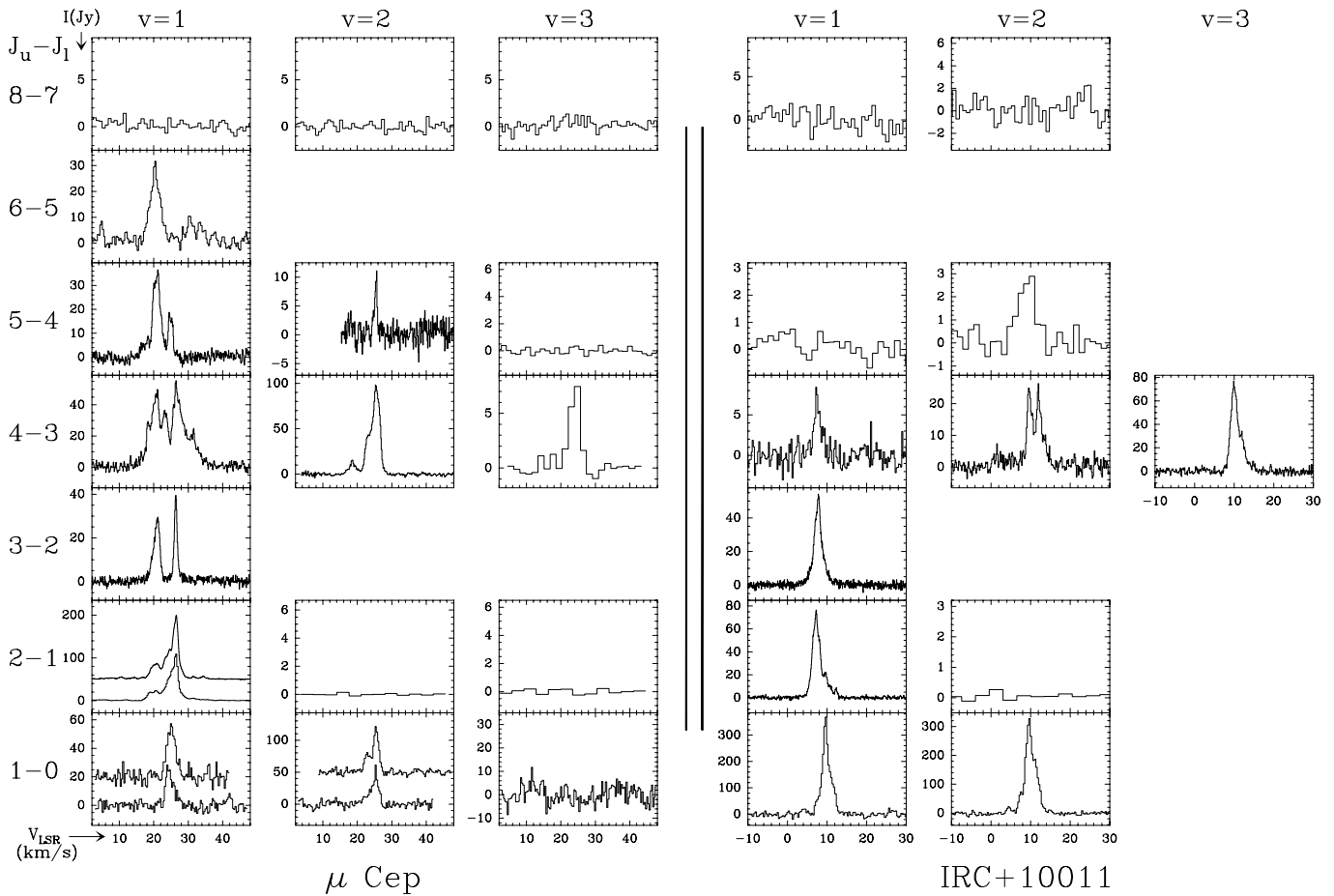


**Fig. 5.** Simultaneous observations of SiO rotational lines in IRC+10011 and  $\mu$  Cep. For  $\mu$  Cep, observations were achieved during November 1992 except a few in January 1993.

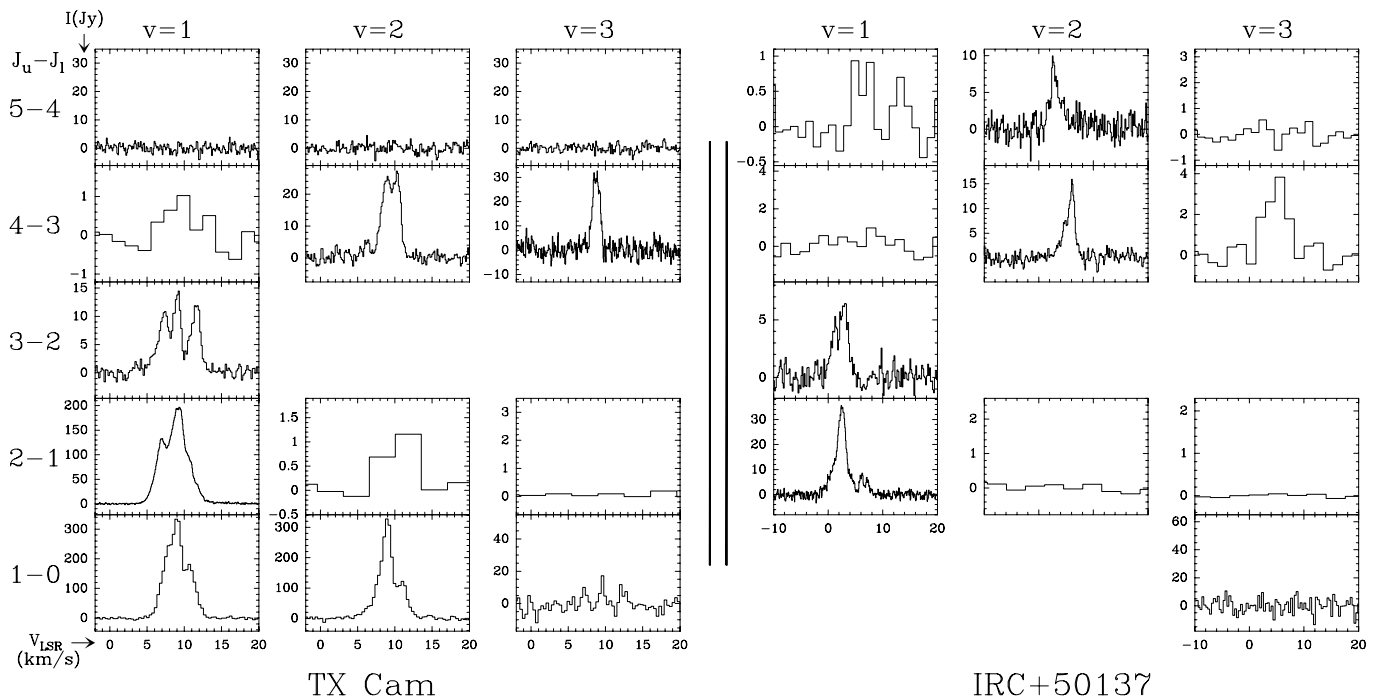


**Fig. 6.** Simultaneous observations of SiO rotational lines in TX Cam and IRC+50137.

emission from inner pulsating layers is probably required to explain those high-velocity wings (see discussion in Cernicharo et al. 1997).

As already found by Cernicharo et al. (1993) for the red supergiant VY CMa, we observe in the objects of our sample a very high contrast between the  $v=3$ ,  $J=4 \rightarrow 3$  emission and that of other rotational lines inside  $v=3$ . As we have pointed out above, standard calculations for both radiative (IR from the central star) and collisional pumping give small contrast between adjacent rotational lines inside a given  $v$ . Our observations indicate that such property is only roughly satisfied for the  $v=1$  lines of  $^{28}\text{SiO}$ . We also note that the  $v=2$  and  $v=3$   $J=4 \rightarrow 3$  lines are stronger than the  $v=1$   $J=4 \rightarrow 3$  one in half of the observed objects (NML Cyg, S Per, IRC+10011, IRC+50137, TX Cam, R Aql and R Cas).

Another well known anomaly is the very weak emission (or even the lack of emission) of the  $^{28}\text{SiO}$   $v=2$   $J=2 \rightarrow 1$  line. Our observations confirm it: we find only tentative detections in TX Cam and RR Aql. Olofsson et al. (1981) proposed that the occurrence of an overlap between the IR line of  $^{28}\text{SiO}$   $v=1$ ,  $J=0 \rightarrow v=2$ ,  $J=1$  and the  $\nu_2=0$ ,  $12_{7,5} \rightarrow \nu_2=1$ ,  $11_{6,6}$  line of water vapor could overpopulate the  $v=2$ ,  $J=1$  level of  $^{28}\text{SiO}$  and, hence, avoid the  $v=2$ ,  $J=2 \rightarrow 1$  maser to pump. Further discussion of the effect of this overlap can be found in a recent work by Bujarrabal et al. (1996). New detections of this line in S stars by these authors further confirm the proposed overlap as responsible of the mentioned anomaly.

#### 4. Discussion

Some of the observed lines display, in our sample of stars, a regular behavior that can be understood in terms of standard radia-

tive or collisional pumping mechanisms (Bujarrabal, 1994-I-II; Locket & Elitzur, 1992). The SiO  $v=1$  lines in IK Tau constitute a clear example of this regular behavior. They show similar line profiles and an intensity variation from one rotational transition to the next of at most a factor 4–5. We are most interested, however, in those cases that cannot be explained in terms of the classical theoretical models (the best known is the lack of maser emission in the  $v=2$   $J=2 \rightarrow 1$  line of  $^{28}\text{SiO}$  and the strong maser emission in the  $v=2$   $J=1 \rightarrow 0$  line, as our observations confirm). At the present time this type of behavior, the strong variation of intensity between rotational lines belonging to the same  $v$ -state, has found a unique explanation: it is the natural consequence of overlaps between IR lines belonging to the same or to different molecules.

Line overlaps between IR ro-vibrational lines may strongly perturbate the radiative pumping of the associated rotational levels. When two IR lines overlap, the stronger one will emit photons that will be absorbed by the other (thinner) overlapped line, so that this excess of photons will modify the equilibrium populations of the involved upper and lower levels of the transition. On the other hand, the stronger overlapping line will absorb photons emitted by the star, reducing the available radiation field at the frequency of the other line (relative to the hypothetical case in which overlap does not occur), and therefore decreasing the number of absorption events in this transition. We note that these two effects are opposite, and that the preponderance of one or the other will depend in general on source geometry. Thus the effect of overlaps is complex, although we can expect that, in case of a very thick line overlaps with an optically thin one, the excitation of the former line will remain essentially unchanged, while the other line will experiment drastic changes

**Table 3.** Non-detected  $^{28}\text{SiO}$  lines

object	Limit $3\sigma$ (Jy)								
	v1 J=4-3	v1 J=5-4	v1 J=6-5	v1 J=8-7	v2 J=1-0	v2 J=2-1	v2 J=5-4	v2 J=8-7	v3 J=1-0
R Aql	D	2.423	8.854	0.978	7.776	0.552	0.446	0.889	
RR Aql	D	D	12.879	0.654	D	D(0.423)	0.722	0.311	23.49
R Cas	D	D	5.033	0.495	D	0.311	1.919	0.418	12.663
TX Cam	1.310	1.102			D	D(???)	1.226		12.690
T Cep	D	D	7.439		D	0.259	1.987		14.526
$\mu$ Cep	D	D	D	0.575	D	0.278	D	0.261	10.935
NML Cyg	D	D	6.093	0.329	9.693	0.203	1.647	0.249	
R Leo	D	D			D	0.321	D		8.667
S Per	1.115	D		0.696	D	0.288	1.498	0.548	12.609
IK Tau	D	D			D	0.354	D		16.146
IRC+10011	D	1.037			D	0.286	D		
IRC+50137	1.443	1.008		0.834		0.444	D	0.572	14.985

object	Limit $3\sigma$ (Jy)								
	v3 J=2-1	v3 J=4-3	v3 J=5-4	v3 J=8-7	v4 J=2-1	v4 J=4-3	v4 J=5-4	v4 J=8-7	v5 J=2-1
R Aql	1.770	D		1.235		1.881	0.923	0.647	0.149
RR Aql	0.510	0.794		1.206		0.675		0.489	
R Cas	0.477	D				1.304		0.512	
TX Cam	0.225	D	0.715						
T Cep	0.383	3.137	1.080	0.639				0.639	
$\mu$ Cep	0.471	D	0.706	0.554		0.453		0.214	
NML Cyg	0.211	2.013		0.668		0.756		0.469	
R Leo	0.165	D	D		0.189	1.881	0.923		0.149
S Per	0.344	D	2.101	0.442		0.414		0.785	
IK Tau	0.236		0.974						
IRC+10011		D							
IRC+50137	0.122	D	1.346						

When “D” is indicated, the line has been observed and detected (see Figs. 1-6). If indication does not appear, the transition has been not observed in the corresponding object. In RR Aql and TX Cam, detection of  $v=2, J=2 \rightarrow 1$  is tentative (tables 12 and 14) and we give here  $3\sigma$  limits for them.

**Table 4.** Infrared overlaps which can affect the rotational lines of  $^{28}\text{SiO}$  from the model presented in González-Alfonso & Cernicharo (1997).

Overlap 1:	$^{28}\text{SiO } v=1-0 J=3-4$	$p\text{-H}_2\text{O } (0,1,0) 7_{3,5}-(0,0,0)7_{6,2}$	$\Delta V = 1.2 \text{ km s}^{-1}$
Overlap 2:	$^{28}\text{SiO } v=2-1 J=6-5$	$o\text{-H}_2\text{O } (0,1,0) 11_{5,6}-(0,0,0)12_{6,7}$	$\Delta V = 8.5 \text{ km s}^{-1}$
Overlap 3:	$^{28}\text{SiO } v=2-1 J=5-4$	$p\text{-H}_2\text{O } (0,1,0) 11_{7,5}-(0,0,0)12_{8,4}$	$\Delta V = 16.3 \text{ km s}^{-1}$
Overlap 4:	$^{28}\text{SiO } v=2-1 J=4-3$	$^{29}\text{SiO } v=1-0 J=1-0$	$\Delta V = 0.6 \text{ km s}^{-1}$
Overlap 5:	$^{28}\text{SiO } v=2-1 J=5-4$	$^{29}\text{SiO } v=1-0 J=2-1$	$\Delta V = 5.0 \text{ km s}^{-1}$

in the pumping of the associated levels. On the other hand, it is not necessary for the overlap to be very close in frequency, because a velocity gradient in the region can couple the lines. A detailed explanation of the effects of overlaps can be found in Olofsson et al. (1985) and in Cernicharo et al. (1991).

Attending to their spectroscopic characteristics and abundances, the molecular species that seem more capable to affect the  $^{28}\text{SiO}$  rotational line intensities are the other stable SiO isotopomers ( $^{29}\text{SiO}$  and  $^{30}\text{SiO}$ ) and water vapor. Cernicharo et al. (1991) have shown that the  $^{29}\text{SiO } v=1 J=4 \rightarrow 3$  maser line is produced by an IR overlap between  $^{29}\text{SiO}$  and  $^{28}\text{SiO}$ . There exists a high number of overlaps between the three SiO isotopomers, and some of them could in principle affect the pumping of the  $^{28}\text{SiO}$  lines (Cernicharo and Bujarrabal 1992, Cernicharo et al. 1993). The models of González-Alfonso & Cernicharo (1997) explain the maser emission in the  $^{28}\text{SiO } v=3$  and  $v=4$  rotational lines

in terms of overlaps between the three SiO isotopomers. Many maser lines of  $^{29}\text{SiO}$  and  $^{30}\text{SiO}$  have been also explained by the same authors. On the other hand, Olofsson et al. (1981, 1985) attributed the lack of emission in the  $^{28}\text{SiO } v=2 J=2 \rightarrow 1$  line to the overlap between  $^{28}\text{SiO } v=2 J=1 \rightarrow v=1 J=0$  and  $para\text{-H}_2\text{O } (0,1,0) 12_{75} \rightarrow (0,0,0) 11_{66}$  (see also Bujarrabal et al., 1996). We shall restrict to the above molecular species in order to try to qualitatively explain the anomalies in the rotational transitions of  $^{28}\text{SiO}$  found in the present study. Table 4 lists those overlaps that could be at the origin of such effects.

As we have pointed out above, the main anomalies within  $v=1$  correspond to the  $J=4 \rightarrow 3$  and  $J=5 \rightarrow 4$  relative intensities. We note that the populations of the associated rotational levels could be affected by various overlaps. First, the overlap number 1 in Table 4 with  $para\text{-H}_2\text{O}$  is able to overpopulate the  $v=1 J=3$  level of  $^{28}\text{SiO}$ , increasing the intensities of the  $v=1 J=3 \rightarrow 2$  and

$J=5\rightarrow 4$  lines relative to the  $J = 4 \rightarrow 3$ . The strong water line  $(0,1,0) 11_{5,6} \rightarrow (0,0,0) 12_{6,7}$ , if seen in absorption (transferring molecules to the  $J=5, v=1$  level of  $^{28}\text{SiO}$ ), could also increase the intensity of  $^{28}\text{SiO } v=1 J=5\rightarrow 4$ . Such behavior is evident in RR Aql and S Per.

The strong overlap number 4 in Table 4 ( $0.6 \text{ km s}^{-1}$ ) could be considered a candidate to affect appreciably the populations of the  $^{28}\text{SiO}$  levels involved, thus explaining the anomalous high emission of the  $^{28}\text{SiO } v=2 J=4\rightarrow 3$  line in most of the stars of our sample. However, since the  $^{29}\text{SiO}$  line involved in overlap 4 is expected to be optically thin, the possible influence of such overlap on the populations of the  $^{28}\text{SiO}$  levels would be considered doubtful (see also González-Alfonso & Cernicharo, 1997). The above is the main anomaly found in the  $v=2$  state of  $^{28}\text{SiO}$ , taking apart the lack of emission in the  $v=2 J=2\rightarrow 1$  line. Only in IRC+50137, both the  $v=2 J=4\rightarrow 3$  and  $J=5\rightarrow 4$  lines show similar intensities, but they are clearly shifted in velocity (see fig 6). We have not a satisfactory explanation for this anomaly: if overlap number 4 has no significant effect on the  $^{28}\text{SiO}$  level populations, only overlap 3 in Table 4 could affect the level populations associated to the  $v=2 J=4\rightarrow 3$  and  $J=5\rightarrow 4$  transitions. If the strong water line in overlap 3 is seen in absorption, the  $v=2 J=5\rightarrow 4$  line would be weaker relative to the  $J = 4 \rightarrow 3$  line. However, the velocity shift of the lines in overlap 3 is  $\approx 16 \text{ km s}^{-1}$ , what precludes this overlap to work in most of the observed objects.

Finally, the overlap number 5 between  $v=1, J=2\rightarrow v=0, J=1$  of  $^{29}\text{SiO}$  and  $v=2, J=5\rightarrow v=1, J=4$  of  $^{28}\text{SiO}$  has not probably any appreciable effect on the  $^{28}\text{SiO}$  level populations, because the  $^{29}\text{SiO}$  line is thinner than the  $^{28}\text{SiO}$  one. It seems that the IR overlaps between  $^{28}\text{SiO}$  and  $\text{H}_2\text{O}$  have more influence on the  $^{28}\text{SiO}$  rotational lines of  $v=1$  and  $v=2$  than the overlaps between the SiO isotopomers. However, these effects will strongly depend on the relative fraction of molecules in the  $v=2$  level of  $^{28}\text{SiO}$  and of the  $v=1$  of  $^{29}\text{SiO}$ . For temperatures below 1000 K the ro-vibrational lines of  $^{29}\text{SiO}$  and of  $^{28}\text{SiO}$  involved in these overlaps could have similar opacities. For high- $v$  ro-vibrational lines, like those of the  $v = 3$  and  $v = 4$  masers of  $^{28}\text{SiO}$ , as well as for the rotational lines of  $^{29}\text{SiO}$  and  $^{30}\text{SiO}$  (see González-Alfonso & Cernicharo, 1997), the line opacity ratio is favorable for the presence of strong effects of the overlap on the rotational line excitation. The influence of these IR overlaps is discussed in detail in González-Alfonso & Cernicharo (1997) where they conclude that all these maser lines are pumped through IR overlaps between  $^{28}\text{SiO}$ ,  $^{29}\text{SiO}$  and  $^{30}\text{SiO}$ .

## 5. Conclusions

We have reported simultaneous observations of the  $^{28}\text{SiO}$   $v=1,2,3,4$  rotational emission from  $J=1\rightarrow 0$  up to  $J=8\rightarrow 7$  (only  $J=7\rightarrow 6$  has not been observed in every  $v$  state, as well as  $J=6\rightarrow 5$  and  $J=3\rightarrow 2$  in  $v=2,3$  and 4) in 12 well known SiO emitters. Most observations were performed in 1992 November 14-15, and the rest of them were performed  $\sim 65$  days later. This time interval is short enough to allow line comparisons, taking into account the typical variability period of the observed objects.

The weak emission of the  $J=2\rightarrow 1 v=2$  line has been confirmed in the present observations, but we have reported tentative detections of this line in two stars: RR Aql and TX Cam.

In most objects the lines show spectral features which do not have counterparts neither in lines of other  $v$ -states nor in lines of the same  $v$ -state (see for example the  $v=1, v=2$  lines of T Cep and the  $v=2$  lines of IRC+50137). Emission from half of the objects show similar shapes within  $v=1$ , in agreement with the “maser chains” predicted by simple models of maser excitation. However, in other objects (R Cas being the most remarkable one) no regular pattern is present even within  $v=1$ . It is particularly noticeable the peculiar behavior of the  $v=1 J=5\rightarrow 4$  line. In  $v=2$  and 3, the  $J=4\rightarrow 3$  line, when detected, shows a strong contrast with respect to the other observed lines in the same  $v$ -state. We do not report any detection of  $v=4,5$  rotational lines in our observations.

The  $v=2$  and  $v=3$  lines detected in R Leo show broader emission than  $v=1$  ones. The total velocity coverage is even larger than twice the terminal expansion velocity of the circumstellar matter measured from thermal  $v=0$  SiO and CO emission. This fact has been not observed in any other object.

Some IR overlaps between lines connecting  $^{28}\text{SiO}$  vibrationally excited levels and transitions of  $^{29,30}\text{SiO } v=1\rightarrow 0$  have been pointed out as the possible origin of the anomalies in the  $^{28}\text{SiO}$  high- $J$  rotational lines in vibrationally excited states. Other overlaps concerning  $\text{H}_2\text{O}$  and  $^{28}\text{SiO}$  IR lines could play a significant role on certain line intensity anomalies, particularly in the cases of the  $^{28}\text{SiO } v=2, J=2\rightarrow 1$  and  $v=1, J=4\rightarrow 3$  ones.

*Acknowledgements.* J.R. Pardo gratefully acknowledges the financial support of the *Observatoire de Paris-Meudon* and the use of its facilities during the development of this work. He also acknowledges the *NASA Goddard Institute for Space Studies* (New York) where the final part of this work has been achieved. We also thank the Spanish DGICYT that has partially supported this work, under projects **PB93-0048** and **ACP96-0168, ESP96-2529-E**.

## References

- Alcolea J., Bujarrabal V., Gallego J.D., 1989, A & A 211, 187.
- Alcolea J., Bujarrabal V., 1992, A & A 253, 475
- Alcolea J., Tesis Doctoral / Universidad Autonoma de Madrid, 1992.
- Alcolea J., Pardo J.R., Bujarrabal V., 1997, in preparation.
- Bujarrabal V., 1994-I, A & A 285, 953.
- Bujarrabal V., 1994-II, A & A 285, 971.
- Bujarrabal V., Alcolea J., Sánchez-Contreras C., Colomer, F., 1996, A & A 314, 883.
- Cernicharo J., 1985, ”ATM, a program to compute atmospheric opacities between 0 and 1000 GHz”, IRAM internal report.
- Cernicharo J., 1988, Thèse de doctorat d’État, Université de Paris VII.
- Cernicharo J., Bujarrabal V., Lucas R., 1991, A & A 249, L27.
- Cernicharo J., Bujarrabal V., 1992, ApJ 401, L109.
- Cernicharo J., Bujarrabal V., Santarén J.L., 1993, ApJ 407, L33.
- Cernicharo J., Brunswig W., Paubert G., Liechti S., 1994, ApJ 423, L143.
- Cernicharo J., Alcolea J., Baudry A., González-Alfonso E., A & A , 1997, A & A 319, 607.
- Cho S.H., Kaifu N., Ukita N., 1996, A & AS 115, 117

- Deguchi S., Good J., Fan Y., Mao X., Wang D., Ukita N., 1983, *ApJ* 264, L65
- González-Alfonso E., Alcolea J., Cernicharo J., 1996, *A & A*, 313, L13
- González-Alfonso E., Cernicharo J., 1997, *A&A*, 322, 938.
- González-Alfonso E., Cernicharo J., Pardo J.R., 1998, in preparation.
- Gray M.D., Ivison, R.J., Yates, J.A., Humphreys, E.M.L., Hall, P.J., Field, D., 1995, *MNRAS*, 277, L67.
- Jewell P.R., Dickinson, D.F, Snyder, L.E., Clemens D.P., 1987, *ApJ* 323, 749-755.
- Kholopov P.N. *et al*, 1985, "General Catalogue of Variable Stars", 4th ed. Moscow.
- Locket, P., Elitzur, M. 1992, *ApJ*, 399, 704.
- Martínez A., Bujarrabal V., Alcolea J., 1988, *A & AS* 74, 273.
- Olofsson H., Rydbeck O.E., Lane A.P., Predmore C.R., 1981, *ApJ* 247, L81.
- Olofsson H., Rydbeck O.E., Nyman L.A., 1985, *A & A* 150, 169.
- Pardo J.R., Thèse de doctorat (Université Pierre et Marie Curie [Paris VI] - Universidad Complutense de Madrid), 1996.
- Pijpers F.P, Pardo J.R., Bujarrabal V., 1994, *A & A* 286, 501.